6 Evidence for $K\pi$-atoms

Y. Allkofer, C. Amsler, A. Benelli[5], S. Horikawa, C. Regenfus, and J. Rochet

in collaboration with:
CERN, Czech Technical University, Institute of Physics ACSR and Nuclear Physics Institute ASCR (Czech Republic), Laboratori Nazionali di Frascati, Messina University, Trieste University, KEK, Kyoto Sangyo University, Tokyo Metropolitan University, IFIN-HH (Bucharest), JINR (Dubna), Skobeltsin Institute for Nuclear Physics (Moscow), IHEP (Protvino), Santiago de Compostela University, Basel University, Bern University.

(DIRAC-II Collaboration)

Electromagnetically bound $\pi^{\mp}K^{\pm}$-pairs ($\pi^{\mp}K^{\pm}$-atoms) have been observed for the first time in 2008 by our DIRAC-II Collaboration at CERN (1; 2). The π^+K^--atom is unstable and decays through the strong force into $\pi^0\bar{K}^0$ (while π^-K^+-atoms decay into π^0K^0). The mean life τ, which we intend to measure, is related to the S-wave πK-scattering lengths a_1 and a_3 in the isospin 1/2 and 3/2 states, respectively. The πK-scattering length is of interest to test chiral perturbation theories extended to the s-quark.

Predictions for τ can be obtained from the S-wave phase shifts of the πK-system, extrapolated to low energy kaon-nucleon scattering ($\pi K \to \pi K$ scattering off the exchanged π). However, kaon-nucleon scattering at low momentum is difficult due to the short lifetime of the kaon and hence the S-phase shifts are poorly known at low energy. The experimental uncertainties in a_1 and a_3 are correspondingly substantial, and the predicted mean life of πK-atoms scatters between 1 and 5 fs. Using the values from dispersion relations (3) one predicts a mean life $\tau \sim 3.7$ fs.

Details on the previous apparatus (DIRAC-I) to study $\pi^+\pi^-$-atoms (4) can be found in ref. (5). A sketch of the modified spectrometer (DIRAC-II) to collect the πK (and more $\pi\pi$) data is shown in Fig. 6.1. The 24 GeV/c proton beam from the CERN-PS impinges on a

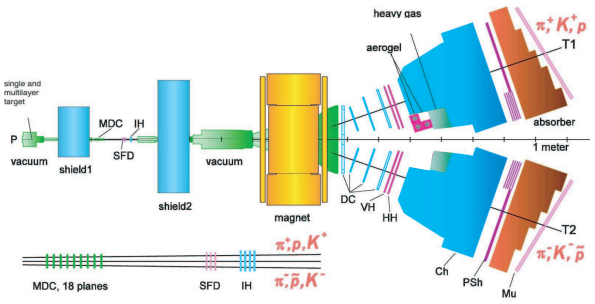

Figure 6.1: Sketch of the updated DIRAC-II spectrometer, showing the locations of the Čerenkov counters to identify electrons, pions and kaons. MDC = microdrift chambers, SFD = scintillator fibre detector, IH = ionization hodoscope, DC = drift chambers, VH, HH = vertical and horizontal scintillation hodoscopes, PSh = preshower, Mu = muon counters.

26 μm Pt-target (average intensity of 1.6×10^{11} protons/pulse). The proton beam then passes through a vacuum pipe and is absorbed by the beam dump. The secondary particles emerging from the target are analyzed in a double-arm magnetic spectrometer measuring the momentum vectors of two oppositely charged hadrons. The particles are collimated through two steel shielding blocks, upstream of the microdrift chambers (MDC) and downstream of the ionization hodoscope (IH), respectively. They pass through a vacuum chamber and are bent by the 1.65 T field of the dipole magnet. The two-arm spectrome-

[5]Visitor from the University of Basel

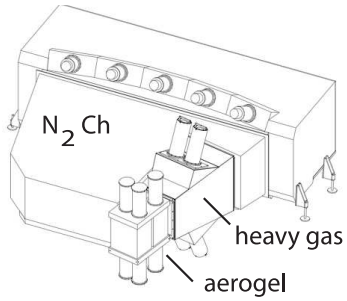

Figure 6.2:
N_2, aerogel and heavy gas Čerenkov counters.

ter is tilted upwards with respect to the proton beam by an angle of 5.7°. Positive particles are deflected into the left arm, negative ones into the right arm. Electrons and positrons are vetoed by the N_2-Čerenkov detectors (Fig. Fig. 6.2) and muons by their signals in scintillation counters behind the steel absorbers. Pions are separated from kaons with the heavy gas and aerogel counters. The signal from πK-atoms is observed for kaon and pion pairs with a very small relative momentum (typically $|Q_L| < 3$ MeV/c is the c.m.s system).

The Zurich group carries the main responsibility for the πK measurements, while the rest of the collaboration concentrates on $\pi\pi$. Our group has developed and built a novel aerogel Čerenkov counter in the left arm (positive charges) for kaon detection and proton suppression, and the heavy gas system for pion detection. An aerogel detector in the right arm (negative charges) is not necessary since the antiproton flux is negligible compared to that from negative kaons, while protons in the left arm are much more frequent than positive kaons. The aerogel detector consists of three independent modules. Two of them (total volume of 24ℓ) have refractive index $n = 1.015$ for kaons between 4 and 5.5 GeV/c, and the third one (13ℓ) has the lower index $n = 1.008$ for 5.5 to 8 GeV/c kaons and kaon-proton separation. The loss due to light absorption is compensated by using a wavelength shifter and by increasing the radiator thickness in the center of the detector (pyramid geometry). Details can be found in our recent publications (6; 7) and in previous annual reports.

The startup of DIRAC-II, originally planned for summer 2006, was postponed by one year due to repeated failures of a switching magnet in the CERN primary proton beam line. The defective magnet was successfully replaced in spring 2007 and DIRAC-II could be commissioned in June 2007. The aerogel counters worked according to expectations and data were taken in 2007 and 2008.

Last year the Zurich group was involved in the data analysis of the runs taken so far. This includes test beam calibrations and Monte-Carlo simulation for the aerogel counter. An event preselection was performed for both the πK and the $\pi\pi$ data. We studied the energy loss in the detector for the various particles and thereby cured a longstanding small momentum shift in the Q_L-distribution. We now describe the analysis of the 2007 data which led to the first observation of πK-atoms (1; 2).

For this analysis we used only detectors downstream of the dipole magnet. The trajectories were determined by the drift chambers, the pattern recognition starting from the coordinates in the last plane and extrapolating back to the target. The variable of interest in the following analysis is the relative momentum Q of the $\pi^{\mp}K^{\pm}$-pairs in their center-of-mass systems, in particular the longitudinal component Q_L which is not affected by multiple scattering. In the transverse plane, the resolution on the relative momentum Q_T (typically 3 MeV/c) is dominated by multiple scattering, while the resolution on the longitudinal component Q_L (< 1 MeV/c) is not affected. For further analysis we use therefore only Q_L.

Figure 6.3 shows the four mechanisms which contribute to the production of $\pi^{\pm}K^{\mp}$-pairs. Accidental pairs are due to particles produced on different nucleons (Fig. 6.3a), non-Coulomb-pairs are associated with the production of long-lived intermediate states

(Fig. 6.3b). On the other hand, $\pi^{\pm}K^{\mp}$-pairs which interact electromagnetically form correlated Coulomb-pairs (Fig. 6.3c), or atomic bound states (Fig. 6.3d). The latter atoms, while traveling through the target, can either decay, be (de)-excited or break up into $\pi^{\pm}K^{\mp}$-pairs which emerge from the target with very low relative momentum.

For prompt pairs the time difference between the positive and negative spectrometer arm lies between –0.5 and 0.5 ns. Accidental pairs are first removed using the time information from the vertical hodoscopes. Accidental pairs (those with large time differences) are also needed for subsequent analysis. Electrons or muons are removed, and a loose preselection of oppositely charged particles is performed (2). Pions, kaons and protons below 2.5 GeV/c can be separated by time-of-flight. For the $\pi^{-}K^{+}$ analysis the aerogel detector is used in addition to remove protons in the positive arm, while for the $\pi^{+}K^{-}$ analysis the time difference between the negative and the positive arm has to be negative to remove protons faking pions.

Once the accidentals have been subtracted the prompt pairs are composed of the following three types: atomic-pairs, Coulomb-pairs, and non-Coulomb-pairs. We assume that the background due to non-Coulomb pairs can be described by the Q_L-distribution of accidentals, following a similar analysis for $\pi^{+}\pi^{-}$-atoms (4). Coulomb pairs have to be simulated. Since the shapes of both contributions are known, one can extrapolate into the $|Q_L| < 3$ MeV/c signal region. The difference (residuals) between the data and the sum of both contributions is plotted in Fig. 6.4. Above $|Q_L| = 3$ MeV/c the residuals are consistent with zero, while the enhancement at low relative momentum is the first evidence for πK-atoms. We obtain 173 $\pm$ 54 detected atomic pairs with a statistical significance of 3.2σ. The systematic uncertainty is estimated to be around 5%, much smaller than the statistical one.

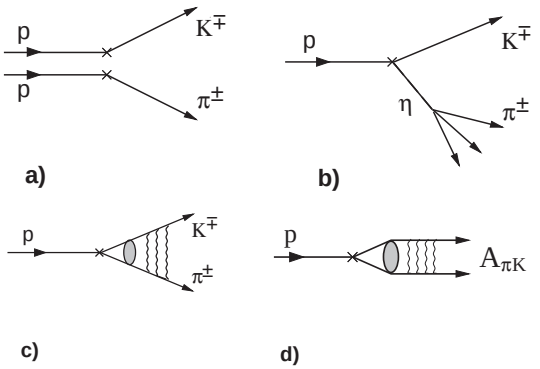

Figure 6.3:
Production mechanisms of πK-pairs: a) accidental-pairs from two protons; b) non-Coulomb-pairs from long-lived intermediate states such as the η-meson; c) Coulomb-pairs from direct production or from short-lived intermediate states; d) πK-atoms.

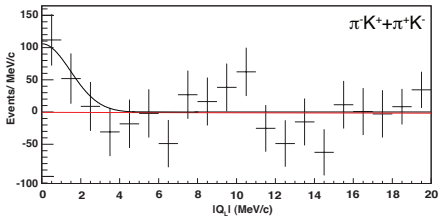

Figure 6.4:
Residuals between data and the fitted background for $\pi^{-}K^{+}$ and $\pi^{+}K^{-}$. A Gaussian fit has been applied (solid line) to illustrate the distribution of atomic-pairs.

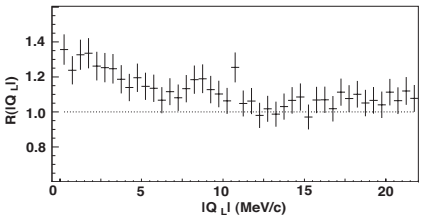

Figure 6.5:
Correlation function R as a function of $|Q_L|$ for πK-pairs. The deviation from the horizontal dotted line proves the existence of Coulomb-πK-pairs.

The evidence for the observation of πK-atoms is strengthened by the observation of Coulomb-pairs which, a fortiori, implies that atoms have also been produced. This can be seen as follows: non-Coulomb pairs have a similar Q_L-distribution as accidentals. Hence

dividing the normalized distribution for prompt pairs by the one for accidentals one obtains the correlation function R describing Coulomb-pairs. The function R, shown in Fig. 6.5 as a function of $|Q_L|$, is clearly increasing with decreasing momentum, proving that Coulomb-pairs have been observed.

The ratio of the number of produced atoms to the number of Coulomb-pairs with small relative momenta has been calculated (8; 9). This number needs to be corrected by Monte-Carlo simulation to take into account the acceptance of the apparatus and the cuts applied in the analysis. The breakup probability P_{br} relates the number of atoms to the number of atomic pairs. A calculation of the breakup probability as a function of mean life (Fig. 6.6) has been performed using the Born approximation (10). For the predicted mean life of 3.7 fs P_{br} is 53% (dotted line in Fig. 6.6). One then obtains from the number of produced atoms the predicted number of observed atomic pairs, 147 $\pm$ 36, in good agreement with the experimental result.

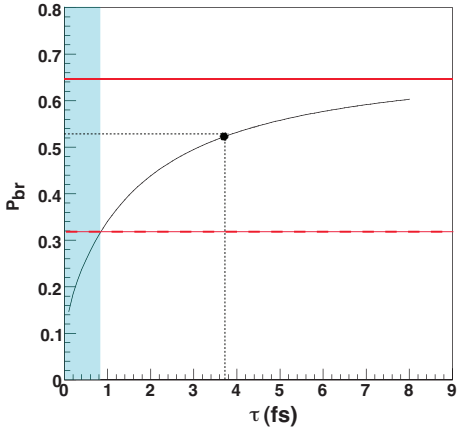

Figure 6.6: Breakup probability P_{br} for the 26 μm Pt-target as a function of mean life of πK-atoms in the 1s-state. The horizontal solid line is the measured breakup probability and the horizontal dashed line the 1.28σ lower bound corresponding to a lower limit of 0.8 fs for the mean life. The excluded area (90% confidence level) is shown in blue. The horizontal dotted line gives the theoretical prediction corresponding to 3.7 fs.

Conversely, one can use the number of observed atomic-pairs from the fit and the number of Coulomb-pairs below $|Q_L| < 3$ MeV/c to calculate the breakup probability: P_{br} = 64 $\pm$ 25 % (horizontal solid line in Fig. 6.6). This leads to a lower limit for the mean life of πK-atoms of τ_{1S} = 0.8 fs at a confidence level of 90%. This result can be translated into an upper limit $|a_{1/2} - a_{3/2}| < 0.58\ m_\pi^{-1}$ at 90% confidence level.

The choice of Pt as production target for the 2007 data was justified by the high breakup probability so that of πK-atoms could be observed. Data taken in 2008 – 2010 are being collected with a 98 μm Ni-target, for which the breakup probability is lower ($\sim$35% according to ref. (10)) but still rapidly rising around the predicted mean life of 3.7 fs. This will allow a more accurate measurement of τ. The ultimate goal is to measure the mean life of πK-atoms with a precision of about 20%, leading to a 10% uncertainty in the difference of scattering lengths $|a_{1/2} - a_{3/2}|$.

[1] B. Adeva et al. (DIRAC Collaboration), Phys. Lett. **B 674** (2009) 11.

[2] Y. Allkofer, PhD Thesis, University of Zurich (2008).

[3] P. Büttiker, S. Descotes-Genon, B. Moussallam, Eur. Phys. J. **C 33** (2004) 409.

[4] B. Adeva et al. (DIRAC Collaboration), Phys. Lett. **B 619** (2005) 50.

[5] B. Adeva et al. (DIRAC Collaboration), Nucl. Instr. Meth. in Phys. Res. **A 515** (2003) 467.

[6] Y. Allkofer et al., Nucl. Instr. Meth. in Phys. Res. **A 582** (2007) 497; Y. Allkofer et al., Nucl. Instr. Meth. in Phys. Res. **A 595** (2008) 84.

[7] S. Horikawa et al., Nucl. Instr. Meth. in Phys. Res. **A 595** (2008) 212.

[8] L.L. Nemenov, Sov. J. Nucl. Phys. **41** (1985) 629.

[9] L. Afanasyev and O. Voskresenskaya, Phys. Lett. **B 453** (1999) 302.

[10] B. Adeva et al., CERN-SPSC-2004-009, SPSC-P-284, Add.4.